Bioorganic & Medicinal Chemistry Letters 29 (2019) 1985–1993

Contents lists available at ScienceDirect

Bioorganic & Medicinal Chemistry Letters

journal homepage: www.elsevier.com/locate/bmcl

Synthesis and structure activity relationships of a series of 4-amino-1*H*-pyrazoles as covalent inhibitors of CDK14

Fleur M. Ferguson[a,b,1], Zainab M. Doctor[a,b,1], Scott B. Ficarro[a,c,d], Jarrod A. Marto[a,c,d,e], Nam Doo Kim[f], Taebo Sim[g,h], Nathanael S. Gray[a,*]

[a] Department of Cancer Biology, Dana-Farber Cancer Institute, Boston, MA 02215, USA
[b] Department of Biological Chemistry and Molecular Pharmacology, Harvard Medical School, Boston, MA 02215, USA
[c] Blais Proteomics Center, Dana-Farber Cancer Institute, Boston, MA 02215, USA
[d] Department of Pathology, Brigham and Women's Hospital, Harvard Medical School, Boston, MA 02215, USA
[e] Department of Oncologic Pathology, Dana-Farber Cancer Institute, Boston, MA 02215, USA
[f] Daegu-Gyeongbuk Medical Innovation Foundation, Republic of Korea
[g] Chemical Kinomics Research Center, Korea Institute of Science and Technology, Republic of Korea
[h] KU-KIST Graduate School of Converging Science and Technology, Korea University, Republic of Korea

ARTICLE INFO

Keywords:
Covalent kinase inhibitor
CDK14
TAIRE kinase
CDK15
CDK16
CDK17
CDK18
CDK inhibitor
Mitosis
Cell cycle

ABSTRACT

The TAIRE family of kinases are an understudied branch of the CDK kinase family, that have been implicated in a number of cancers. This manuscript describes the design, synthesis and SAR of covalent CDK14 inhibitors, culminating in identification of FMF-04-159-2, a potent, covalent CDK14 inhibitor with a TAIRE kinase biased selectivity profile.

Introduction

CDK14 is a member of the understudied TAIRE subfamily of cyclin-dependent kinases, named after the "TAIRE" sequence motif in their cyclin binding site, and comprising of CDKs 14–18.[1–3] CDK14 overexpression has been reported in numerous cancers including colorectal cancer,[4] ovarian cancer[5] and gastric cancer.[6] However, selective tool compounds to interrogate the pharmacological consequences of CDK14 inhibition were, until recently, unavailable.

We recently reported the identification and characterization of FMF-04-159-2 (**100**), the first covalent CDK14 inhibitor with TAIRE-kinase bias.[7] Off-target CDK2 activity was identified, and experimental conditions to minimize CDK2 engagement and maximize CDK14 engagement were reported.[7] Here we describe the structure activity relationships of a series of 4-amino-1*H*-pyrazole analogs for CDK14 biochemical and cellular potency, and measure their effects on HCT116 proliferation. We show cellular engagement of CDK14 by lead molecules, and demonstrate their covalent nature by MS/MS studies. This data is of interest, as 4-amino-1*H*-pyrazole is a widely used kinase inhibitor scaffold.[8] This SAR analysis aids development of further, improved CDK14 inhibitors, and in addition, provides insight into how CDK14 activity can be removed from 4-amino-1*H*-pyrazole analogs targeted towards other kinases.

In search of chemical leads for CDK14, we performed a CDK14 cellular engagement screen of a library of reported CDK inhibitors using a biotin JNK-IN-7 pulldown assay.[9] This identified the multi-targeted CMCG kinase inhibitor AT7519 as an efficient CDK14 inhibitor at 1 μM.[10] This result was confirmed using a LanthaScreen CDK14 binding assay (Table 1).

SiRNA mediated CDK14 knockdown does not cause significant proliferation defects in the HCT116 cell line, unlike knockdown of other CDK kinases.[11] A selective CDK14 inhibitor is consequently also expected to have mild to insignificant effects on HCT116 cell growth. Therefore we used potency in a CellTiter-Glo (Promega) proliferation

* Corresponding author.
E-mail address: nathanael_gray@dfci.harvard.edu (N.S. Gray).
[1] These authors contributed equally.

https://doi.org/10.1016/j.bmcl.2019.05.024
Received 3 April 2019; Received in revised form 14 May 2019; Accepted 14 May 2019
Available online 23 May 2019

Table 1
Single ring R^1 analogs of AT7519. A) CDK14 IC_{50}s were measured using a LanthaScreen binding assay. IC_{50}s were calculated as the average of three replicates, and are reported ± the standard errorB) Antiproliferative activity against the HCT116 cell line was measured using a CellTiter-Glo assay. IC_{50}s were calculated as the average of three replicates, and are reported ± the standard error.

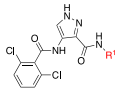

Compound	R^1	R^2	IC_{50} CDK14 (nM)	IC_{50} HCT116 (nM)	Compound	R^1	R^2	IC_{50}CDK14 (nM)	IC_{50} HCT116 (nM)	Compound	R^1	R^2	IC_{50}CDK14 (nM)	IC_{50} HCT116 (nM)
AT7519		–	19.8 ± 2.8	132 ± 33	15		H	479 ± 102	737 ± 200	20	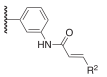	CH_2NMe_2	88 ± 13	723 ± 352
11	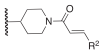	H	401 ± 60	341 ± 97	16		CH_2NMe_2	977 ± 421	1341 ± 412	21	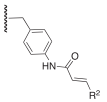	H	> 1000	117 ± 41
12	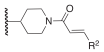	CH_2NMe_2	208 ± 40	1053 ± 309	17		H	> 1000	17 ± 6	22	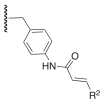	CH_2NMe_2	108 ± 53	4700 ± 130
13		H	569 ± 121	39 ± 10	18		CH_2NMe_2	82 ± 10	395 ± 102	23	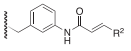	H	ND	8500 ± 3700
14		CH_2NMe_2	148 ± 66	157 ± 38	19	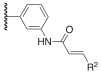	H	> 1000	169 ± 55	24	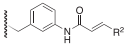	CH_2NMe_2	183 ± 49	> 10,000

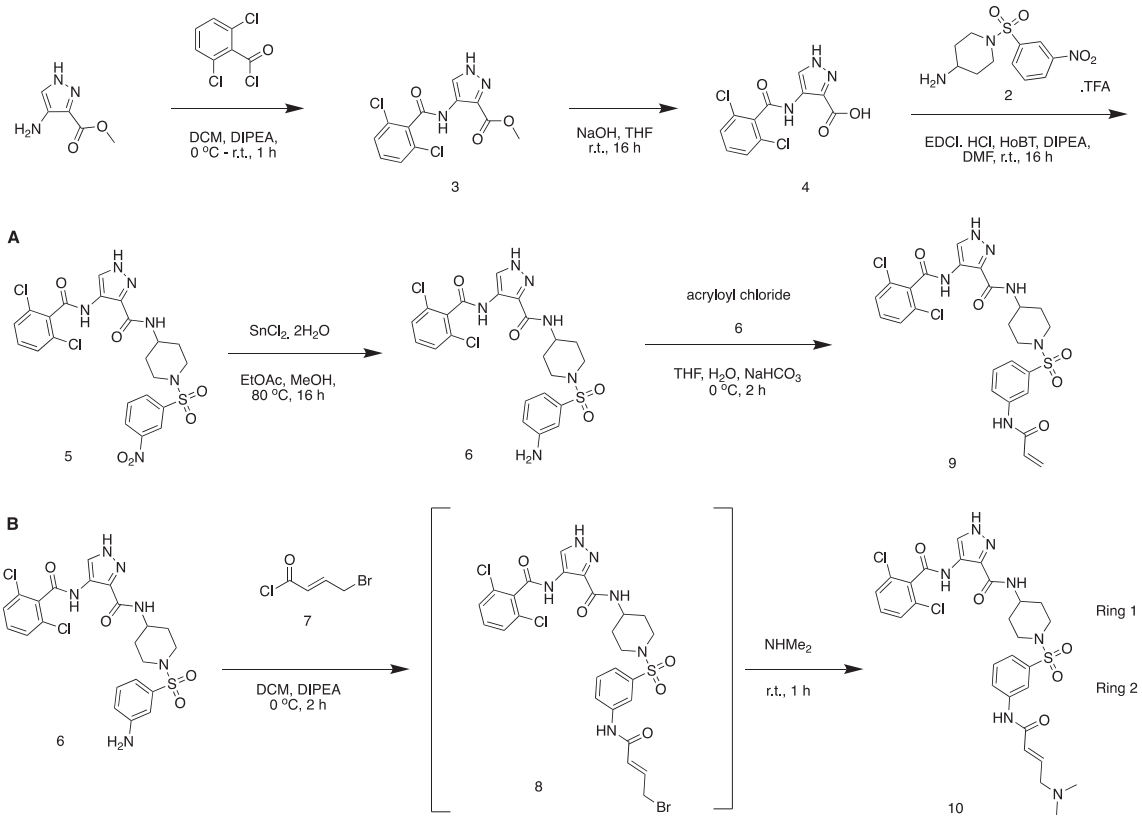

Scheme 1. Representative synthesis of 4-amino-1*H*-pyrazole analogs. See also supporting information.

assay as a first pass approximation of compound selectivity for CDK14 when prioritizing molecules for progress through further rounds of characterization (Supporting Fig. 1). As previously reported, AT7519 is a potent inhibitor of HCT116 cell proliferation, with an IC_{50} of 132 nM.[7]

CDK14 contains a uniquely placed cysteine, C218, located at the beginning of the αD helix, proximal to the ATP pocket.[12] In order to improve the potency and selectivity of AT7519 towards CDK14, we sought to design a covalent inhibitor. Examination of the co-crystal structure of CDK2 in complex with AT7519 (PDB: 2VU3) revealed that the 4-aminopiperidine is oriented towards the αD helix in CDK2.[10] Assuming a conserved binding mode, this substituent (R^1) should provide a suitable vector for targeting CDK14 C218. Therefore, analogs containing varied R^1 substituents incorporating acrylamide and (*E*)-4-(dimethylamino)but-2-enamide warheads (R^2) were synthesized according to Scheme 1.

Initially, molecules containing a single saturated or unsaturated ring were synthesized (Table 1, compounds **11–24**). These analogs lost significant potency relative to AT7519, potentially due to the loss of a hydrogen bonding interaction with the piperidine NH seen in CDK2 (PDB:2VU3), which was not compensated for by covalent inhibition.

JNK3 contains a cysteine in an equivalent region of the kinase to CDK14. Examination of the structure of JNK3 in complex with JNK-IN-7 (PDB: 3V6S) indicated that a longer distance between the hinge binding motif and the acrylamide is required in order to successfully form a covalent bond.[9] Therefore analogs were prepared containing two linked cyclic aliphatic or aromatic rings decorated with acrylamide or (*E*)-4-(dimethylamino)but-2-enamide warheads (Table 2, **25-70**). Docking studies into a CDK14 homology model built from the X-ray structure of CDK12 (PDB: 4NST) predicted that a range of linked two ring systems, with 1,4-regiochemistry in ring 1 and a 1,3-regiochemistry in ring 2 would best allow for C218 covalent engagement (Fig. 1).[7,13]

Molecules containing a piperidine linked to an aminobenzamide at R^1 displayed reduced potency for CDK14 relative to AT7519 (Table 2, **25–32**). 1,4 aminopiperidine regiochemistry at R^1 is strongly preferred, with 1,3 aminopiperidine regiochemistry not well tolerated at this position (e.g. **27** vs **31**). Preference for a 1,3 aminobenzamide regiochemistry of the second ring was observed with the most potent analogs, **27** and **28**, combining these two regiochemistries, in line with computational docking results.

Replacing the aminobenzamide (**28**) with an aminobenzylamine (**36**) dramatically increased potency against CDK14. Again, a strong preference for a 1,4 aminopiperidine regiochemistry and a 1,3 aminobenzylamine regiochemistry was observed (Table 2, **36** vs **34**). The most potent analogs, **35** and **36**, inhibited CDK14 with IC_{50}s below 1 nM in the LanthaScreen biochemical assay. **36** was chosen for follow-up studies due to its lower toxicity in the cell titer glo assay, relative to **35**. Both compounds show increased toxicity relative to AT7519, indicating off-target activity. Compounds containing an aminobenzylsulfonamide followed similar trends to the aminobenzamide series. Compound **36** is highly potent against CDK14, and also displays increased toxicity against HCT116 cells (see Fig. 2).

Inspired by the acrylamide bearing substituent in JNK-IN-7, amide linked biphenyls were introduced to R^1 (Table 1 compounds **43–52**).[9] Although these compounds displayed reduced affinity, they also exhibited the same regiochemical preferences. Interestingly in this series, the *E*)-4-(dimethylamino)but-2-enamide warhead was preferred to the acrylamide warhead. **46** was the most potent of this subseries against CDK14, but also had increased toxicity relative to AT7519.

In an attempt to improve selectivity in a manner analogous to JNK-IN-8, compounds were synthesized with *ortho*-methylation of the 1,4-diaminoaniline in ring 1 (**47, 48**). Unfortunately, this methylation was not tolerated by CDK14. Substitution of the ring 1 piperidine group for a pyrrolidine resulted in compounds with a less favorable CDK14 :

Table 2
Extended R^1 analogs of AT7519. A) CDK14 IC_{50}s were measured using a LanthaScreen binding assay. IC_{50}s were calculated as the average of three replicates, and are reported ± the standard errorB) Antiproliferative activity against the HCT116 cell line was measured using a CellTiter-Glo assay. IC_{50}s were calculated as the average of three replicates, and are reported ± the standard error. –R is used to denote reversible control compounds (without an alkene group).

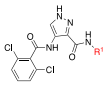

Compound	R^1	R^2	IC_{50} CDK14 (nM)	IC_{50} HCT116 (nM)	Compound	R^1	R^2	IC_{50} CDK14 (nM)	IC_{50} HCT116 (nM)	Compound	R^1	R^2	IC_{50} CDK14 (nM)	IC_{50} HCT116 (nM)
AT7519		–	19.8 ± 2.8	132 ± 33	40	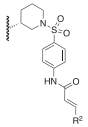	CH_2NMe_2	ND	> 10,000	58	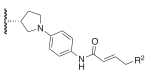	H	> 1000	2900 ± 940
25	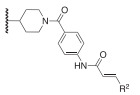	H	126 ± 21	42 ± 11	41	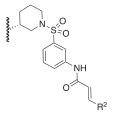	H	836 ± 321	> 10,000	59	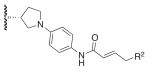	CH_2NMe_2	117 ± 28	> 10,000
26	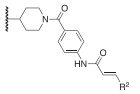	CH_2NMe_2	83 ± 11	404 ± 111	42	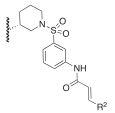	CH_2NMe_2	> 1000	> 10,000	60	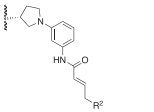	H	> 1000	826 ± 420
27	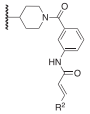	H	45 ± 4	32 ± 10	43	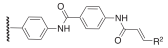	H	169 ± 28	8.3 ± 3.1	61	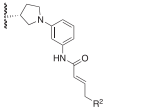	CH_2NMe_2	218 ± 59	> 10,000
28	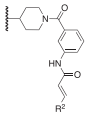	CH_2NMe_2	77 ± 12	485 ± 126	44	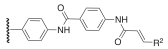	CH_2NMe_2	68 ± 10	14 ± 4	62	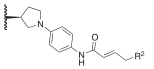	H	267 ± 156	64 ± 15
29	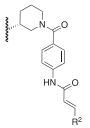	H	ND	726 ± 510	45	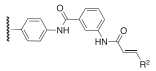	H	> 1000	6.3 ± 3.2	63	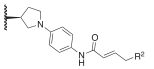	CH_2NMe_2	738 ± 289	714 ± 179
30	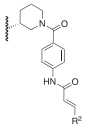	CH_2NMe_2	> 1000	> 10,000	46	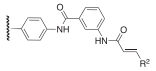	CH_2NMe_2	17 ± 3	38 ± 12	64	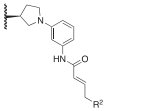	H	> 1000	22 ± 6
31	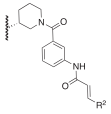	H	> 1000	> 10,000	47	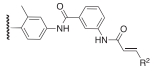	H	> 1000	ND	65	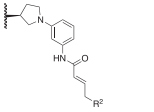	CH_2NMe_2	> 1000	124 ± 33

(*continued on next page*)

Table 2 (*continued*)

Compound	R^1	R^2	IC_{50} CDK14 (nM)	IC_{50} HCT116 (nM)	Compound	R^1	R^2	IC_{50} CDK14 (nM)	IC_{50} HCT116 (nM)	Compound	R^1	R^2	IC_{50} CDK14 (nM)	IC_{50} HCT116 (nM)
32	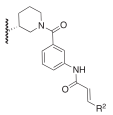	CH_2NMe_2	> 1000	> 10,000	48	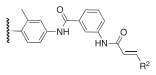	CH_2NMe_2	> 1000	320 ± 94	66	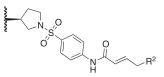	H	> 1000	3000 ± 670
33	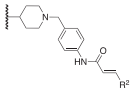	H	10 ± 3	< 1	49	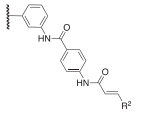	H	ND	6.0 ± 1.5	67	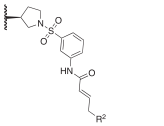	H	> 1000	467 ± 134
34	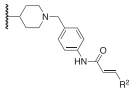	CH_2NMe_2	14 ± 3	2.6 ± 0.9	50	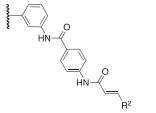	CH_2NMe_2	72 ± 12	24 ± 6	68	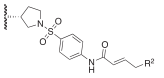	CH_2NMe_2	41 ± 18	> 10,000
35	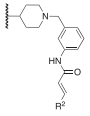	H	< 1	< 1	51	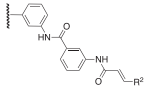	H	308 ± 63	31 ± 12	69	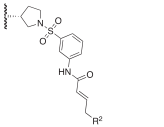	H	450 ± 315	6150 ± 2240
36	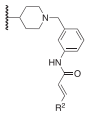	CH_2NMe_2	< 1	2.2 ± 0.9	52	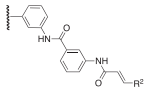	CH_2NMe_2	34 ± 12	367 ± 152	70	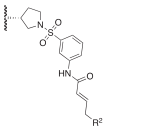	CH_2NMe_2	308 ± 72	> 10,000
37	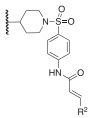	H	62 ± 8	31 ± 10	53	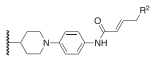	H	154 ± 24	30 ± 10	71	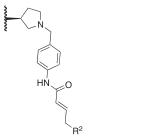	H	257 ± 55	< 1
38	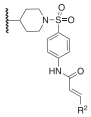	CH_2NMe_2	2.6 ± 0.8	23 ± 6	54	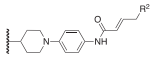	CH_2NMe_2	45 ± 16	541 ± 134	72	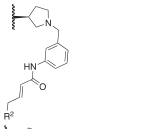	H	282 ± 120	< 1
9	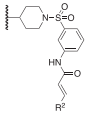	H	< 1	< 1	55	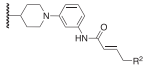	H	ND	93 ± 29	73	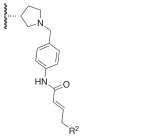	H	572 ± 178	31 ± 8
10	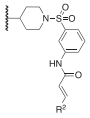	CH_2NMe_2	1.8 ± 0.7	5.1 ± 1.4	56	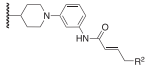	CH_2NMe_2	27 ± 7	427 ± 102	74	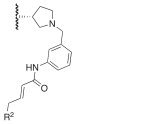	H	151 ± 72	27 ± 8
39	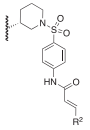	H	> 1000	> 10,000	57	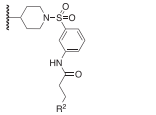	H	11 ± 2	76 ± 11	75	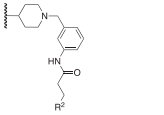	H	82 ± 29	123 ± 38

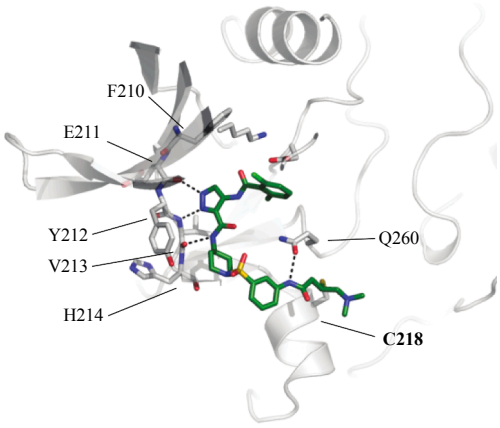

Fig. 1. Docking of compound 10 into a homology model of CDK14. View from above.

HCT116 potency profile (e.g. **72** vs **35)** with the exception of **68**, which was taken forward for validation. Removal of the linking atoms between rings 1 and 2 afforded 3(piperidine-1-yl)anilines **53–56**. This series maintained acceptable CDK14 potency and the dimethylamino-substituted analogs **54** and **56** had low HCT116 toxicity. **56** was chosen for follow up studies.

Finally, the propyl amide analogs of the most potent molecules were synthesized to examine the effects of removal of the covalent warhead. **57** was ~10-fold less potent against CDK14 compared to **9** and **10**, and displayed similar toxicity against HCT116 cells to **10**. Compound **75** was significantly less potent against both CDK14 and HCT116 cells than **35** and **36**. This indicated that the covalent binding component improved binding towards CDK14, but also towards off-targets that alter cell proliferation.

To verify that the 6 lead compounds and two reversible control compounds identified in Table 2 were able to engage CDK14 in cells we performed a pull-down experiment. Cells were treated for 4 h with compounds at various doses, and then lysed and treated with biotinylated JNK-IN-7,[9] followed by streptavidin coated beads. CDK14 capture was assayed by western blot. (Table 3, SI Fig. 1). Of these compounds, **10** was able to potently block CDK14 pulldown at 50 nM, and **36, 46** and **27** also showed effects at 500–1000 nM concentrations (Supporting Fig. 2). Compounds **56** and **68** were not active, or weakly active in the cellular assay (Supporting Fig. 2). The reversible control molecules also showed no activity in this assay, indicating a dependency on covalent bond formation for activity in cells. Covalent bond formation by **10** and **36** was verified by incubating compounds with purified, recombinant CDK14 followed by MS/MS analysis. Both compounds achieved complete labeling of CDK14 when incubated for 3 h at r.t., at a 10:1 M ratio of compound to CDK14/Cyclin Y protein. Digest experiments followed by MS analysis showed that C218 was exclusively labeled.

To evaluate the cellular targets of **10** and **36** more broadly, we performed KiNativ profiling at 1 μM compound concentration (Fig. 1).[14,7] This revealed that whilst both compounds were potent against CDK14, they also inhibited a large number of other kinases.

As hinge binding is a common feature of Type I kinase inhibitors, analogs of FMF-03-198-2 with altered hinge binding motifs predicted to reduce hydrogen bonding interactions were synthesized, in an attempt to increase the selectivity for CDK14 by reducing the reversible binding affinity, but maintaining the ability to bind covalently (Table 4, **76–87).**

Unfortunately, none of these analogs demonstrated potent inhibition in the CDK14 binding assay (Table 4). Therefore, the 2,6-dichlorobenzamide substituent (R^3) was varied in an effort to improve selectivity (Table 5). In the co-crystal structure of AT7519 in complex with CDK2, the 2,6-benzamide group fills a small hydrophobic pocket, and prior studies have demonstrated that CDK2 binding activity can be tuned by altering it's substituents, by introducing steric clashes with the back pocket.[10] Substitution of the 2,6-dichloro phenyl ring of **9** and **10** for a more polar 2,6-difluoro phenyl ring (**88, 89**) yielded a modest reduction in toxicity and maintained potent CDK14 inhibition.

The bulkier 2-chloro, 6-methoxy substitution yielded a further reduction in toxicity, whilst maintaining potency for CDK14 (**90, 91**). The reversible propyl amide **93** maintained comparable potency towards CDK14 and comparable potency against HCT116 cells as **90**, indicating this effect was primarily driven by changes in the reversible binding profile of the compounds. However, further increase in the bulk of the 6-substituent to an ethoxy group afforded a more toxic compound (**92**), indicative of a narrow SAR window at the 6-position. 2,6-dimethoxy substitution (**96**), 2,4,6-methoxy substitution (**104**) and 2,4,6-chloro substitution (**100**) patterns resulted in reduced CDK14 potency, but also dramatically reduced HCT116 toxicity.

Addition of a methoxy group to the 3-position of **10** to afford **97** didn't significantly affect CDK14 binding or toxicity. Finally, the unsubstituted compound **107** exhibited potent CDK14 inhibition and reduced HCT116 toxicity. The active compounds from this series were taken forward for cellular target engagement studies (Table 6, Supporting Fig. 2). Of these, only **91** and **100** were able to completely inhibit CDK14 pull-down at concentrations below 1 μM.

Compound **91** and **100** were both evaluated using the KiNativ platform for cellular selectivity at concentrations of 1 μM and compared to the profiles of **10** and **36**. Compound **91** demonstrated a comparable number of targets compared to **10** and **36**, despite its reduced cytotoxicity. However, compound **100** showed a favorable profile, with a dramatically reduced number of targets.

Of the 6 targets inhibited at > 75%, 4 were TAIRE kinases (CDK14, CDK16, CDK17, CDK18). These kinases have been reported to display functional redundancy, and thus the pan-TAIRE activity of **100** may aid interrogation of the biology of these understudied kinases.[15] The other targets of **100** were CDK2 and CDK10. Despite binding to these off-targets, **100** was demonstrated to engage CDK14 in cellular context much more potently than CDK2, with an IC_{50} of 39.6 nM for CDK14 compared to 256 nM for CDK2, as measured by the NanoBRET assay.[7] This improved cellular potency for CDK14 over CDK2, and other off-targets of compound **100** offered an improvement in the relative cellular selectivity for CDK14 compared to AT7519. Future work is required to remove activity against these targets from CDK14 / TAIRE kinase probes, therefore use of washout conditions is recommended when using **100** to probe the pharmacological consequences of CDK14 inhibition.[7] Compound **100** represents a significant advance towards developing chemical probes for the TAIRE kinase family, and is the first targeted covalent CDK14 inhibitor.

Table 3
Cellular target engagement of lead compounds in biotin pull-down assay, estimated based on testing of three compound concentrations.

Compound	IC_{50} CDK14 (nM)	Compound	IC_{50} CDK14 (nM)
9	1000	46	1000
36	500	10	50
75	> 1000	57	> 1000
56	1000	68	> 1000

Table 4

FMF-03-198 analogs with a modified heterocyclic core. A) CDK14 IC_{50}s were measured using a LanthaScreen binding assay. IC_{50}s were calculated as the average of three replicates, and are reported ± the standard error. B) Antiproliferative activity against the HCT116 cell line was measured using a CellTiter-Glo assay. IC_{50}s were calculated as the average of three replicates, and are reported ± the standard error.

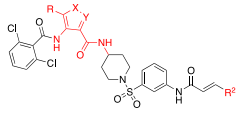

Compound	Scaffold	R^2	IC_{50} CDK14 (nM)	IC_{50} HCT116 (nM)	Compound	Scaffold	R^2	IC_{50} CDK14 (nM)	IC_{50} HCT116 (nM)	Compound	Scaffold	R^2	IC_{50} CDK14 (nM)	IC_{50} HCT116 (nM)
9		H	< 1	< 1	79		H	> 1000	563	84		H	> 1000	9200 ± 3000
10		CH_2 NMe_2	1.8 ± 0.7	5.1 ± 1.4	80		CH_2 NMe_2	> 1000	3045	85		CH_2 NMe_2	> 1000	> 10,000
76		H	> 1000	> 10,000	81		H	> 1000	> 10,000	86		H	> 1000	> 10,000
77		CH_2 NMe_2	487 ± 249	> 10,000	82		CH_2 NMe_2	> 1000	> 10,000	87		CH_2 NMe_2	> 1000	> 10,000
78		CH_2 NMe_2	> 1000	> 10,000	83	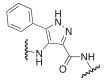	CH_2 NMe_2	> 1000	> 10,000					

Table 5
FMF-03-198 analogs with varied R^3 substituents. A) CDK14 IC_{50}s were measured using a LanthaScreen binding assay. IC_{50}s were calculated as the average of three replicates, and are reported ± the standard error. B) Antiproliferative activity against the HCT116 cell line was measured using a CellTiter-Glo assay. IC_{50}s were calculated as the average of three replicates, and are reported ± the standard error. –R is used to denote reversible control compounds (without an alkene group).

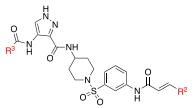

Compound	R^3	R^2	IC_{50} CDK14 (nM)	IC_{50} HCT116 (nM)	Compound	R^3	R^2	IC_{50} CDK14 (nM)	IC_{50} HCT116 (nM)	Compound	R^3	R^2	IC_{50} CDK14 (nM)	IC_{50} HCT116 (nM)
9		H	< 1	< 1	94		H	1.6 ± 2.5	9 ± 3	102		H	ND	7 ± 2
10		CH_2NMe_2	1.8 ± 0.7	5.1 ± 1.4	95		CH_2NMe_2	ND	174 ± 49	103		CH_2NMe_2	ND	90 ± 22
88		H	> 1000	114 ± 41	96		CH_2NMe_2	50 ± 33	4100 ± 1200	104		H	48 ± 33	> 10,000
89		CH_2NMe_2	3.4 ± 2.7	157 ± 48	97		H	0.4 ± 1.5	1.4 ± 1.2	105		CH_2NMe_2	221 ± 91	> 10,000
90		H	2.2 ± 5.3	115 ± 37	98		CH_2NMe_2	6.4 ± 6.6	23 ± 8	106		H	315 ± 182	382 ± 156
91		CH_2NMe_2	3.0 ± 2.8	524 ± 165	99		H	49 ± 11	25 ± 13	107		CH_2NMe_2	3 ± 20	440 ± 112
92		CH_2NMe_2	ND	102 ± 34	100		CH_2NMe_2	88 ± 10	1140 ± 190	108		CH_2NMe_2	332 ± 126	8200 ± 990
93		H	0.8 ± 1.8	173 ± 33	101		CH_2NMe_2	139 ± 10	5900 ± 1200	109		CH_2NMe_2	14 ± 5	395 ± 131

Table 6
Cellular target engagement of additional lead compounds in biotin pull-down assay, estimated based on testing of three compound concentrations.

Compound	IC_{50} CDK14 (nM)	Compound	IC_{50} CDK14 (nM)
91	50	96	> 1000
100	500	104	> 1000
107	1000	101	> 1000

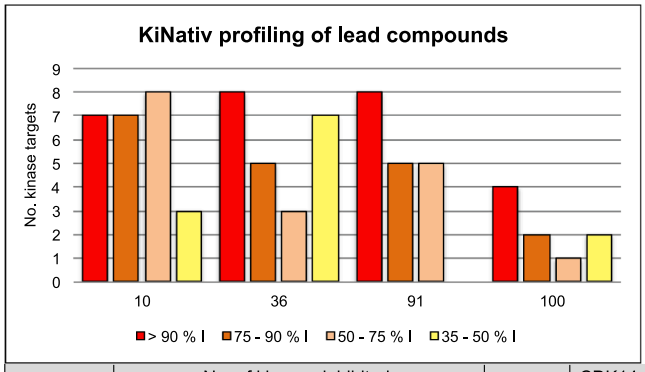

Compound	No. of kinases inhibited				Total	CDK14
	> 90 % I	75 - 90 % I	50 - 75 % I	35 - 50 % I		> 90 % I
10	7	7	8	3	25	Y
36	8	5	3	7	23	Y
91	8	5	5	0	18	N
100	4	2	1	2	9	Y

Fig. 2. KiNativ profiling results of lead compounds at 1 μM compound concentration. % I, percent inhibition relative to DMSO only control.

Acknowledgement

This work was funded by the following grants; R21CA188881, R01CA219850, DFCI Strategic Research Initiative, United States.

Disclosures

J.A.M. is a member of the SAB of Devices. N.S.G. is a founder, SAB member, and equity holder in Gatekeeper, Syros, Petra, C4, B2S, and Soltego. The Gray lab receives or has received research funding from Novartis, Takeda, Astellas, Taiho, Jansen, Kinogen, Her2llc, Deerfield, and Sanofi. N.S.G., F.M.F., and Z.M.D. are inventors on a patent application covering chemical matter in this publication owned by Dana-Farber Cancer Institute. S.B.F, N.D.K. and T.S. have no conflicts to declare

Appendix A. Supplementary data

Supplementary data to this article can be found online at https://doi.org/10.1016/j.bmcl.2019.05.024.

References

1. Fedorov O, Muller S, Knapp S. The (un)targeted cancer kinome. *Nat Chem Biol.* 2010;6:166–169.
2. Fleuren ED, Zhang L, Wu J, Daly RJ. The kinome 'at large' in cancer. *Nat Rev Cancer.* 2016;16:83–98.
3. Malumbres M. Cyclin-dependent kinases. *Genome Biol.* 2014;15:122.
4. Zhu J, Liu C, Liu F, Wang Y, Zhu M. Knockdown of PFTAIRE Protein Kinase 1 (PFTK1) inhibits proliferation, invasion, and EMT in colon cancer cells. *Oncol Res.* 2016;24:137–144.
5. Zhang W, Liu R, Tang C, et al. PFTK1 regulates cell proliferation, migration and invasion in epithelial ovarian cancer. *Int J Biol Macromol.* 2016;85:405–416.
6. Yang L, Zhu J, Huang H, et al. PFTK1 promotes gastric cancer progression by regulating proliferation, migration and invasion. *PLoS ONE.* 2015;10:e0140451.
7. Ferguson FM, Doctor ZM, Ficarro SB, et al. Discovery of covalent CDK14 inhibitors with Pan-TAIRE family specificity. *Cell chemical biology.* 2019;26:1–14.
8. Dimova D, Bajorath J. Assessing scaffold diversity of kinase inhibitors using alternative scaffold concepts and estimating the scaffold hopping potential for different kinases. *Molecules (Basel, Switzerland).* 2017;22.
9. Zhang T, Inesta-Vaquera F, Niepel M, et al. Discovery of potent and selective covalent inhibitors of JNK. *Chem Biol.* 2012;19:140–154.
10. Wyatt PG, Woodhead AJ, Berdini V, et al. Identification of N-(4-piperidinyl)-4-(2,6-dichlorobenzoylamino)-1H-pyrazole-3-carboxamide (AT7519), a novel cyclin dependent kinase inhibitor using fragment-based X-ray crystallography and structure based drug design. *J Med Chem.* 2008;51:4986–4999.
11. McDonald 3rd ER, de Weck A, Schlabach MR, et al. Project DRIVE: a compendium of cancer dependencies and synthetic lethal relationships uncovered by large-scale, Deep RNAi Screening. *Cell.* 2017;170(577–592):e510.
12. Chaikuad A, Koch P, Laufer SA, Knapp S. The Cysteinome of protein kinases as a target in drug development. *Angew Chem Int Ed Engl.* 2018;57:4372–4385.
13. Bosken CA, Farnung L, Hintermair C, et al. The structure and substrate specificity of human Cdk12/Cyclin K. *Nat Commun.* 2014;5:3505.
14. Patricelli MP, Nomanbhoy TK, Wu J, et al. In situ kinase profiling reveals functionally relevant properties of native kinases. *Chem Biol.* 2011;18:699–710.
15. Davidson G, Shen J, Huang YL, et al. Cell cycle control of wnt receptor activation. *Dev Cell.* 2009;17:788–799.